Development and Characterization of New Environmentally Friendly Polylactide Formulations with Terpenoid-Based Plasticizers with Improved Ductility

J. Gomez-Caturla[1] · R. Tejada-Oliveros[1] · J. Ivorra-Martinez[1] · D. Garcia-Sanoguera[1] · R. Balart[1] · D. Garcia-Garcia[1]

Abstract

This work addresses the potential of two biobased terpenoids, linalyl acetate and geranyl acetate, as environmentally friendly monomeric plasticizers for polylactide (PLA). Plasticized formulations of PLA containing 10 wt.% and 20 wt.% terpenoids were melt-compounded in a twin-screw co-rotating extruder and, subsequently, processed by injection moulding for further characterization. In addition, a reactive extrusion process (REX) was carried out on plasticized formulations containing 20 wt.% terpenoids with dicumyl peroxide to anchor the plasticizer molecules into the PLA backbone. Both terpenoids led to a remarkable plasticization effect on PLA, with a noticeable increase in ductile properties. In particular, the elongation at break of PLA, around 4.7%, was improved to values above 230% for all the plasticized formulations, even for low terpenoid concentration of 10 wt.%. Terpenoids also provide increased crystallinity because polymers chains have more mobility and are more readily arranged. This was observed by shifting the cold crystallization process to lower temperatures. As with other monomeric plasticizers, a clear decrease in the glass transition temperature from 61.5 °C (neat PLA), to values of around 40 °C for the plasticized formulations with 20 wt.% terpenoid was obtained. The obtained formulations show high potential since the plasticization efficiency of these terpenoids is very high, thus leading to new toughened-PLA formulations with improved ductility.

Keywords Poly(lactide) (PLA) · Plasticizer · Terpenoids · Reactive extrusion · Ductility

Introduction

Environmental issues such as petroleum depletion, the increase in the carbon footprint, global warming, greenhouse emissions, and life cycle assessment (LCA) are leading to important changes in how we conceive, produce, use, and remove materials. Petroleum-derived polymers and additives have been widely used over the past decades due to their low cost, enhanced durability, easy processing, and a wide range of properties [1], but with a high environmental impact due to the huge amount of generated wastes. To provide a more sustainable polymer industry, research has focused on two main topics related to their synthesis and/or disposal [2].

In the last years, the commercialization of polymers and/or additives from natural resources has risen. These include fully or partially biobased polymers such as polyethylene-PE, polypropylene-PP, polyamide-PA, polycarbonate-PC, polyethylene terephthalate-PET, polyurethane-PU, and so on [3–7]. These polymers offer similar properties to their corresponding petroleum-derived counterparts, including non-biodegradation. On the other hand, a promising group of biobased and biodegradable polymers has risen in the last years. This group includes natural polymers such as polysaccharides, *i.e.* starch, cellulose, chitin (and its derivative, chitosan), pectin [8–10], as well as protein-based polymers such as gluten, casein, ovalbumin, bean proteins (soy, faba, alubia) [11–15], among others. Moreover, bacterial polyesters or polyhydroxyalkanoates-PHAs offer promising applications [16, 17], as well as some other petroleum-based polyesters that are susceptible to disintegration in controlled compost soil, such as polybutylene succinate-PBS, polyglycolide-PGA, poly-ε-caprolactone-PCL, polybutylene succinate-*co*-adipate-PBSA and so on [18–21]. Polylactide

✉ R. Tejada-Oliveros
rateol@epsa.upv.es

1 Institute of Materials Technology (ITM), Universitat Politècnica de València (UPV), Plaza Ferrándiz Y Carbonell 1, 03801 Alcoy, Alicante, Spain

(PLA) is the most promising commercially available aliphatic polyester [1]. PLA can be obtained by direct polycondensation of lactic acid or, more commonly, by ring-opening polymerization (ROP) of lactide, obtained after fermentation of starch-rich compounds [22]. Despite it offers good processability and rather balanced properties, its mechanical, chemical, and physical properties are inferior to traditional petroleum-derived polymers. One of the main drawbacks of PLA is its low ductility, with an elongation at break typically lower than 10%, leading to low toughness [23]. To overcome this, different strategies have been proposed. Blending is one of the most interesting alternatives. A wide range of flexible polymers have been blended with PLA with and without compatibilizers, *i.e.* polyurethanes (PUs), polyethylene-*co*-glycidyl methacrylate (PE-*co*-GMA), polyethylene (PE), polypropylene (PP), poly-ε-caprolactone (PCL) and polybutylene adipate-*co*-terephthalate (PBAT) [24–27].

A second approach is plasticization. Plasticizers also provide PLA with improved biodegradation properties, as reported by Arrieta et al. [28]. Polyethylene glycol (PEG) with different molecular weights has been extensively used as a plasticizer for PLA, as it shows exceptional miscibility [29, 30]. Citrate esters such as triethyl citrate (TEC) and acetyl tributyl citrate (ATBC) have been widely used as plasticizers in PLA formulations, exhibiting excellent ductile properties. Maiza et al. [31] reported plasticized PLA formulations with up to 30 wt.% TEC or ATBC with a noticeable decrease in the glass transition temperature (T_g). Adipate esters have also been widely used in PLA plasticization [32].

Recently, new biobased plasticizers for aliphatic polyesters have been proposed, such as those derived from terpenes. Terpenes include a group of natural products that consist of repeated isoprene (C_5H_8) units, while terpenoids are terpenes with additional functional groups (usually oxygen-containing groups). Esterifying alcohol-based terpenoids with carboxylic acids leads to terpenoid esters with increased interest in polyester plasticization. Terpenes and terpenoids are commonly employed as fragrance chemicals in scented products with additional antibacterial and wound-healing properties [33, 34]. Aside from camphor ($C_{10}H_{16}O$), a naturally-occurring terpenoid, which was the first industrial plasticizer, there is little recent literature regarding the potential of terpene-based compounds as environmentally friendly plasticizers. Arrieta et al. [35] reported the potential of limonene, a natural terpene, as a biobased plasticizer for PLA, showing great plasticization efficiency.

Moreover, terpenes contain one or more unsaturated carbon–carbon bonds that an organic peroxide can activate. Brüster et al. [36] reported the potential of limonene and myrcene as plasticizers for PLA processed by conventional and reactive extrusion (REX), followed by injection moulding. They also concluded that REX is an interesting strategy to obtain balanced plasticization properties

without compromising other mechanical properties. Mangeon et al. [37] have reported the potential of several terpenoids, namely geraniol (G), linalool (L) and geranyl acetate (GAc), as plasticizers for PHB with an interesting but limited increase in elongation at break. Although terpenes have proved to be suitable plasticizers for PLA, the chemical structure of terpenoids and their derivatives (mainly their esters from different carboxylic acids) suggest they could provide improved plasticization properties to PLA. In this work, for the first time, the high plasticization efficiency of two terpenoid esters, namely linalyl acetate (LAc) and geranyl acetate (GAc), on polylactide (PLA) formulations with improved ductility is reported. Moreover, this research assesses the potential of reactive extrusion (REX) with the terpenoid esters mentioned above to attach the plasticizers molecules onto the polylactide backbone. Mechanical, thermalthermomechanical, crystallinity and morphological properties are studied as a function of the plasticizer content and reactive extrusion process. These plasticized-PLA materials could prove to be effective in applications within the packaging sector, for example in the food industry, helping to preserve safety, quality and extending the shelf life of packaged foods during storage and consumption. The plasticizers would increase the ductility of PLA, improving its mechanical properties to produce a more suitable biodegradable packaging product, as those kind of products need sufficient flexibility and resilience [38].

Experimental

Materials

PLA from Total Corbion (Gorinchem, The Netherlands) grade PURAPOL L130 with a melt flow index of 16 g/10 min (ISO 1133-A 210 °C/2.16 kg) was employed. Linalyl acetate and geranyl acetate were purchased from Sigma-Aldrich (Steinheim am Albuch, Germany) with CAS numbers 115-95-7 and 105-87-3. Finally, dicumyl peroxide (DCP) was purchased from Sigma-Aldrich (Lyon, France) with a CAS number 80-43-3. The chemical structure of the employed materials is represented in Fig. 1, and the formulations employed in the experiments are summarized in Table 1.

Theoretical Framework of PLA/Plasticizer Solubility

An essential issue in plasticization is the solubility of the selected plasticizer into the polymer matrix. To this end, the group contribution method proposed by Van Krevelen and Hoftyzer was used to calculate the solubility parameter (δ) and its main contributions related to the dispersion and polar forces, represented by δ_d and δ_p, respectively, and the

Fig. 1 Scheme of the chemical structures of polylactide (PLA), terpenoid-based plasticizers, i.e. linalyl acetate (LAc) and geranyl acetate (GAc), and free radical initiator, dicumyl peroxide (DCP) for reactive extrusion (REX)
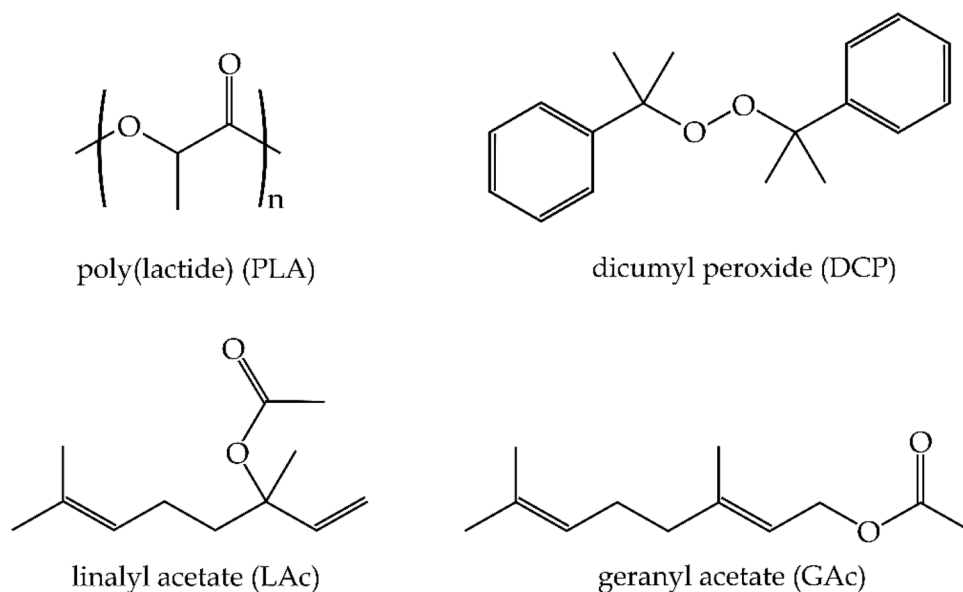
poly(lactide) (PLA)

dicumyl peroxide (DCP)

linalyl acetate (LAc)

geranyl acetate (GAc)

Table 1 Composition of plasticized poly(lactide) formulations with terpenoid-based plasticizers processed by conventional and reactive (REX) extrusion

Code	PLA (wt.%)	Linalyl acetate (LAc) (wt.%)	Geranyl acetate (GAc) (wt.%)	DCP (phr)*
PLA	100			
PLA-10LAc	90	10		
PLA-20Lac	80	20		
PLA-20LAc-DCP	80	20		1
PLA-10GAc	90		10	
PLA-20GAc	80		20	
PLA-20GAc-DCP	80		20	1

*phr stands for parts per hundred resin in the blend

contribution of hydrogen bonding (δ_h). These parameters are related through Eq. 1).

$$\delta = \delta_d^2 + \delta_p^2 + \delta_h^2 \qquad (1)$$

As proposed by Van Krevelen and Hoftyzer, the different components of the solubility parameter may be predicted from group contributions as indicated by Eqs. 2, 3, 4:

$$\delta_d = \frac{\sum F_{di}}{V} \qquad (2)$$

$$\delta_p = \frac{\sqrt{\sum F_{pi}^2}}{V} \qquad (3)$$

$$\delta_h = \sqrt{\frac{\sum E_{hi}}{V}} \qquad (4)$$

Based on the molar attraction constants, the F-method is rather accurate for predicting the dispersive and polar contributions (δ_d, and δ_p, respectively) as mentioned above. Nevertheless, it does not apply to the hydrogen bonding contribution (δ_h). To this, Hansen indicated that the hydrogen bonding energy (E_{hi}) per structural group is almost constant. By taking into account the structure and the group contribution defined by Van Krevelen and Hoftyzer [39], the solubility parameters and their corresponding components are summarized in Table 2. Table 2 also includes the R_a values, which stand for the distance between the solubility coordinates of the plasticizer with regard to PLA and have been calculated using Eq. 5.

$$R_a = \sqrt{4 \cdot (\delta_{d_{plast}} - \delta_{d_{PLA}})^2 + (\delta_{p_{plast}} - \delta_{p_{PLA}})^2 + (\delta_{h_{plast}} - \delta_{h_{PLA}})^2} \qquad (5)$$

In this equation, the constant × 4 in the first term (meaning doubled values of the dispersion parameter in a 3D plot) was obtained from plots of experimental data to define

Table 2 Main parameters related to the theoretical approach for the solubility between poly(lactide) and terpenoid-based plasticizers

Material	δ_d (MPa$^{1/2}$)	δ_p (MPa$^{1/2}$)	δ_h (MPa$^{1/2}$)	δ (MPa$^{1/2}$)	Ra (MPa$^{1/2}$)	RED
PLA	15.32	8.44	10.98	20.66	–	
Linallyl acetate (LAc)	15.65	2.25	5.67	16.80	8.18	0.764
Geranyl acetate (GAc)	15.96	2.29	5.72	17.11	8.19	0.765

spherical solubility regions instead of spheroidal. When the distance, R_a, equals zero, the plasticizer and the polymer are thermodynamically very similar, leading to an excellent solubility. As expected, the solubility is reduced as the distance becomes more remarkable. It is widely recognized that above a certain distance, the solubility can be considered negligible. This distance corresponds to the polymer radius (or sphere radius), R_0, and defines a spherical solubility region of a polymer. The sphere centre corresponds to the polymer's three solubility parameter coordinates, δ_d, δ_p, and δ_h.

The relative energy difference (RED) was calculated by the ratio between the R_a values and the solubility sphere radius for PLA, R_0, which is 10.7 MPa$^{1/2}$ (see Eq. 6) [40]. As suggested by Eq. 6, the closer the RED value to zero, the better miscibility between PLA and the considered plasticizer. RED values close to 1 are on the borderline, while RED values above 1 suggest poor miscibility. Brüster et al. have reported RED values of 0.93 and 0.99 for limonene and myrcene in PLA-plasticized formulations [36]. Even though the RED values are close to 1, they observed that limonene, with a lower RED value, gave PLA more efficient plasticization than myrcene, which RED value is very close to the solubility borderline.

$$RED = \frac{R_a}{R_0} \tag{6}$$

Processing of Plasticized PLA Formulations

PLA pellets were dried at 60 °C for 48 h in a dehumidifying dryer MDEO from Industrial Marsé (Barcelona, Spain). Materials were weighted and premixed before the extrusion process in a co-rotating twin-screw extruder from Construcciones Mecánicas Dupra S.L. (Alicante, Spain) with a 25 mm diameter and a length/diameter ratio of 24. The temperature profile in the four heated zones was 185 °C – 180 °C – 175 °C – 170 °C from the die to the hopper. The residence time was 2 min. Pelletized materials were introduced in an injection moulding machine 270/70 from Mateu&Solé (Barcelona, Spain) with a temperature profile of 190 °C (injection nozzle) – 185 °C – 180 °C – 175 °C (hopper) and a filling time of 1 s. Tensile test samples of $150 \times 40 \times 10$ mm^3 obtained, as well as impact test samples with dimensions of $80 \times 40 \times 10$ mm^3.

Mechanical Properties of Plasticized PLA Formulations

Universal testing machine ELIB 50 from S.A.E. Ibertest (Madrid, Spain) was employed to obtain the main tensile properties (ISO 527–2:2012), namely tensile modulus (E), maximum tensile strength (σ_{max}), and the elongation at break (ε_b). A 5-kN load cell was used for all tests, and the crosshead speed was set to 20 mm/min. The Shore-D hardness was measured in a 676-D durometer from J. Bot Instruments (Barcelona, Spain) on injection-moulded samples with 4 mm thickness, according to ISO 868:2003. The impact behaviour was measured on injection-moulded rectangular ($80 \times 10 \times 4$ mm^3) subjected to a prior notching type "V-notched" with a radius of 0.25 mm according to ISO 179:2010. A 6-J Charpy pendulum from Metrotec S.A. (San Sebastián, Spain) es used to obtain the impact strength. At least 5 specimens of each plasticized PLA formulations were tested to obtain the main mechanical properties at room temperature; results were averaged, and the standard deviation was calculated.

Morphological Properties of Plasticized PLA Formulations

Morphology of the fractured cross-section of the test samples was analyzed in a field emission scanning electron microscope (FESEM) ZEISS ULTRA 55 from Oxford Instruments (Abingdon, UK), working at an acceleration voltage of 2.5 kV. Before the analysis, a sputtering stage was carried out with gold–palladium alloy under an argon atmosphere in a SC7620 sputter coater from Quorum Technologies Ltd. (East Sussex, UK).

Thermal Properties of Plasticized PLA Formulations

The main thermal properties of the PLA and plasticized PLA formulations were obtained by differential scanning calorimetry (DSC) and thermogravimetry (TGA). The DSC runs allowed obtaining the main thermal transitions (melting peak temperature – T_m, cold crystallization peak temperature – T_{cc}) and the corresponding enthalpies (ΔH_m and ΔH_{cc}, respectively). The maximum degree of crystallinity, χ_{cmax}, was obtained by Eq. 7, where w represents the weight fraction of PLA in the considered formulation, ΔH_m stands for the melting enthalpy, ΔH_{cc} stands for the enthalpy of the cold crystallization transition and ΔH_m^0 stands for the

melting enthalpy of a theoretically fully crystalline PLA, which was assumed to have a value of 93 J/g as reported in the literature [41]. The crystallinity related to the cold crystallization process was also calculated by Eq. 7 by taking ΔH as the cold crystallization enthalpy (ΔH_{cc}).

$$\chi_c(\%) = \frac{\Delta H_m - \Delta H_{cc}}{\Delta H_m^0 \cdot w} \cdot 100 \tag{7}$$

DSC runs were conducted in a Q2000 DSC from TA Instruments (New Castle, DE, USA) under a nitrogen atmosphere (66 mL/min), and an average sample weight in the 5–7.5 mg was used. The thermal cycle consisted of three steps. First, a heating cycle was programmed to remove the thermal history from 30 °C to 200 °C at 10 °C/min. Afterwards, a controlled cooling down to − 40 °C at − 10 °C/min was scheduled. Finally, a second heating cycle was programmed up to 300 °C at 10 °C/min. The thermal stability of the samples was studied by thermogravimetry (TGA). The onset degradation temperature – $T_{5\%}$ (temperature to reach a mass loss of 5%), the maximum degradation rate temperature – T_{deg}, and the residual weight, were collected from the characteristic TGA thermograms. A TG-DSC2 thermobalance from Mettler-Toledo (Columbus, OH, USA) was used. Around 6 mg of each formulation were placed into alumina crucibles and subjected to a heating program from 30 °C to 700 °C at 10 °C/min under an air atmosphere. All thermal tests were carried out in triplicate to obtain reliable results.

Thermo-Mechanical Properties of Plasticized PLA Formulations

Dynamic mechanical thermal analysis (DMTA) tests were carried out in a Mettler-Toledo DMA1 (Columbus, OH, USA) in a single cantilever mode. Samples with dimensions $20 \times 6 \times 3$ mm^3 were subjected to a dynamic deformation with an amplitude of 10 μm, while the frequency for the sinusoidal cycles was 1 Hz. Regarding the heating cycle, tests started at − 100 °C and samples were heated up to 100 °C with a heating rate of 2 °C/min. Measurements were performed in triplicate.

X-Ray Diffraction Characterization of Plasticized PLA Formulations

X-ray diffraction patterns were collected at room temperature using a KRISTALLOFLEX K 760-80F x-ray generator at 40 kV and a 40 mA. The radiation from the Cu Kα target was nickel filtered ($\lambda = 0.154$ nm). The scattering angles (2θ) ranged from 5º to 70° with a step size of 0.05º and a speed rate of 1 º/min. The d-spacing in the crystalline domains of PLA was calculated with Bragg's equation (Eq. 8, where λ

is the wavelength of the applied radiation, and θ stands for the peak angle measured.

$$d = \frac{\lambda}{2 \cdot \sin(\theta)} \tag{8}$$

XRD analysis was done on $10 \times 10 \times 10$ mm^3 samples.

Results and Discussion

Mechanical Properties of Plasticized PLA Formulations

The incorporation of terpenoids as plasticizers into the PLA polymer matrix has a noticeable effect on the mechanical properties, as observed in Table 3. Regarding stiffness, the introduction of geranyl acetate (GAc) and linalyl acetate (LAc) promotes a dramatic decrease in the tensile moduli (E), thus suggesting the typical plasticization phenomenon. While neat PLA shows a relatively high tensile modulus of 3984 MPa, typical of a brittle polymer, this is dramatically reduced to 104 MPa for the plasticized formulation containing 20 wt.% LAc. The addition of plasticizers promotes the enhancement of chain motion. As a result, a decrease in the intensity of Van der Waals forces occurs, and the polymer–polymer interactions are considerably reduced. Typically, this effect gives rise to a decrease in the tensile modulus (E) and the tensile strength (σ_{max}) [42, 43]. In this work, the tensile strength of neat PLA was reduced from 57.0 MPa to 15–16 MPa for all the plasticized PLA formulations. This reduced interaction between the polymer chains also promotes the enhancement of the elongation at break ($\varepsilon_b\%$) with such high values of 298.4% for the plasticized PLA formulation with 10 wt.% LAc. Neat PLA shows the typical brittle behaviour with very low elongation at (4.7%). Both terpenoids significantly plasticize PLA, with an increase in elongation at break comparable or even superior to other widely used PLA plasticizers such as PEG, TEC, ATBC,

Table 3 Mechanical properties of PLA and plasticized PLA formulations with terpenoids in terms of tensile modulus (E), maximum tensile strength (σ_{max}), elongation at break (ε_b), Shore D hardness

Code	E (MPa)	σ_{max} (MPa)	ε_b (%)	Shore D
PLA	3984 ± 56	57.0 ± 1.0	4.7 ± 0.4	80.2 ± 1.6
PLA-10LAc	1347 ± 42	15.9 ± 1.3	298.4 ± 4.6	70.5 ± 2.1
PLA-20LAc	104 ± 7	14.2 ± 0.6	236.0 ± 7.7	65.2 ± 0.9
PLA-20LAc-DCP	362 ± 13	16.2 ± 0.5	253.4 ± 6.5	68.6 ± 1.5
PLA-10GAc	1579 ± 55	16.2 ± 0.3	239.8 ± 6.7	70.1 ± 1.2
PLA-20GAc	193 ± 12	14.5 ± 0.4	215.0 ± 9.4	65.4 ± 1.4
PLA-20GAc-DCP	404 ± 24	16.6 ± 0.4	230.7 ± 7.0	67.8 ± 0.8

and adipates, among others. Another interesting finding is that $\varepsilon_b\%$ is not improved for plasticized PLA formulations with 20 wt.% plasticizer. This means that plasticizer saturation occurs, as reported by Liu et al. [44]. As can be seen in Table 3, the $\varepsilon_b\%$ for the plasticized PLA formulation with 10 wt.% LAc reaches a value of 298.4%, while an increase to 20 wt.% LAc does not improve $\varepsilon_b\%$ and, on the contrary, is decreased down to 236.0%. In terms of the plasticizing effect obtained by both terpenoid-based plasticizers in this work, LAc provides PLA with higher elongation at break than GAc. Using plasticizers with similar chemical structures at the same concentrations can lead to remarkable changes in plasticized PLA formulations, as reported by Burgos et al. [45], in PLA formulations plasticized with three different oligomers of lactic acid (OLAs). In addition to the observed plasticization properties, both terpenoids contain several carbon–carbon double bonds, which could be used to graft the terpenoid-based plasticizer onto the PLA backbone. This can be obtained by reactive extrusion (REX) with an organic peroxide, as reported by Bruester et al. [36] in plasticized PLA formulations with limonene and myrcene. Due to the REX process, they obtained increased tensile strength and modulus. At the same time, the elongation at break was reduced, thus suggesting plasticizer anchorage onto PLA polymeric chains after REX with 2,5-bis(*tert*-butylperoxy)-2,5-dimethylhexane. In the present work, dicumyl peroxide (DCP) was used as a free radical initiator during REX in plasticized PLA formulations containing 20 wt.% LAc and GAc. During the reactive extrusion, the dicumyl peroxide decomposes into cumyloxy radicals that tend to abstract protons from the polymer backbone and plasticizers, as reported by Liao et al. [46]. They proposed a mechanism for the covalent bonding between tannin acetate (with different acetylation degrees) and PLA during REX with low amounts of DCP. This consisted in a first stage in which DCP was decomposed by β-scission to the respective free radical. The formed free radicals then could abstract hydrogen from both PLA polymer chains and tannin acetate (from hydroxyl groups and from benzene rings). After this, the recombination of free radicals led to grafting tannin molecules into the PLA backbone, with a subsequent increase in tensile strength and Young's modulus. Similar effects were obtained through REX of PLA-LAc and PLA-GAc in the presence of DCP. It is worthy to note that all tensile properties are increased by REX with DCP in PLA-LAc and PLA-GAc formulations, thus suggesting that REX is an efficient method to improve both resistant and ductile properties on plasticized PLA formulations. Figure 2 shows a schematic representation of the grafting process of terpenoids onto the PLA backbone. In the first stage, the organic peroxide is decomposed by β-scission into free radicals. These free radicals promote hydrogen abstraction from PLA and terpenoid in the second stage. Finally, recombination of the free radicals on PLA and terpenoid, lead to chemical grafting of the terpenoid molecule into the main PLA backbone.

This behaviour was also observed in Shore D hardness values. The incorporation of LAc and GAc remarkably reduces the initial Shore D hardness of PLA (80.2) to such low values of 65. A clear decreasing tendency can be detected with increasing LAc and GAc content in plasticized PLA formulations. As expected, REX with DCP provided slightly higher Shore D hardness values for both terpenoids used in this research, thus supporting the hypothesis of somewhat anchorage of LAc and GAc molecules onto the PLA backbone by grafting.

Morphological Properties of Plasticized PLA Formulations with Terpenoids

The surface morphology obtained after the fracture of the samples in the tensile test was analyzed by field-emission scanning electron microscopy (FESEM). The results are shown in Fig. 3. The obtained structure changed from a flat surface observed for neat PLA (Fig. 3a), representative of a typical brittle fracture, to a rough surface resulting from plastic deformation, representative of a ductile fracture. As observed in Table 3, the highest value of elongation at break observed in the tensile test was obtained for the PLA-10LAc formulation. This effect was reflected in the surface morphology with the highest roughness with the formation of filament-like structures during fracture (Fig. 3c), as reported by Arrieta et al. in plasticized PLA formulations with limonene [35]. Although the elongation at break is not improved for plasticized formulations containing 20 wt.% of LAc or GAc, which could suggest plasticizer saturation, this phenomenon was not observed by FESEM since phase separation was not detected. As mentioned above, the solubility parameters of PLA, LAc and GAc suggest good solubility between them, which was confirmed by relative energy difference (RED) values lower than 1. Lundberg et al., have reported phase separation phenomena in plasticized PLA films with oligomers of tributyl citrate (TBC). They observed that as the molecular weight of oligomers increased, the saturation threshold was reduced to values of 10–15 wt.%. They did not observe phase separation with TBC.

In contrast, a clear phase separation phenomenon was detected in plasticized PLA formulations containing TBC oligomers (TBC-3 and TBC-7 with molecular weights of 980 and 2240 g/mol, respectively). So, although the elongation at break of PLA-20LAc and PLA-20GAc does not increase with respect to lower plasticizer content formulations, phase separation does not occur due to good miscibility and low molecular weight. As reported by Rojas-Lema et al. [47], phase separation is more common in polymer blends due to the high molecular weight of polymers.

Fig. 2 Schematic representation of the plausible reactions occurring during REX of PLA and terpenoids in presence of dicumylperoxide (DCP)
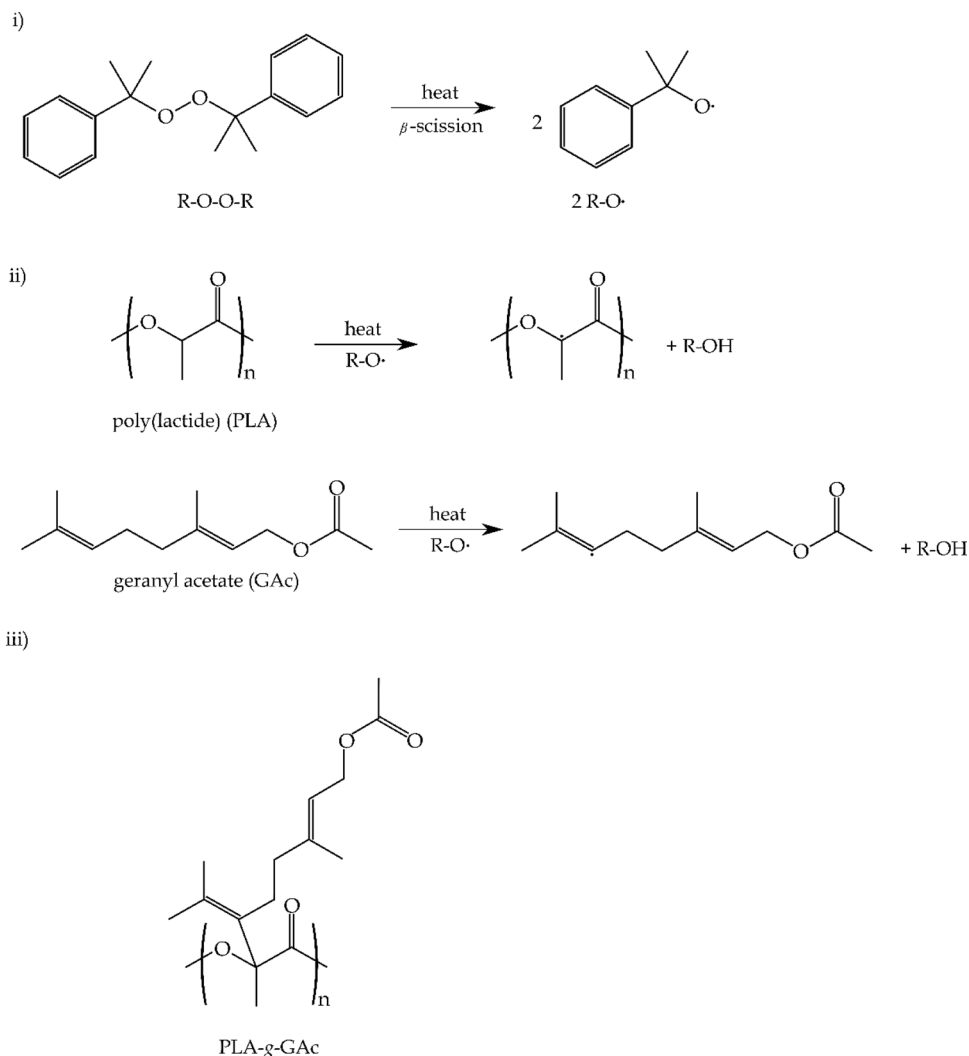

Thermal Properties of Plasticized PLA Formulations with Terpenoids

The main thermal transitions of the PLA and plasticized PLA formulations with LAc and GAc were measured by differential scanning calorimetry (DSC). Figure 4 shows the corresponding thermograms, while Table 4 summarizes the main thermal parameters. After removing the thermal history in the first heating cycle, Fig. 4 gathers the DSC thermograms corresponding to the second heating cycle. The glass transition temperature of neat PLA is 61.5 °C. This is moved down to values of 50.4 °C and 39.5 °C with 10 wt.% and 20 wt.% LAc, respectively, thus showing excellent plasticization efficiency. A similar tendency can be observed for plasticized PLA with GAc, despite the characteristic T_g values being slightly higher than those obtained with LAc. These values are similar to those reported by Maiza et al. [32], in plasticized PLA formulations with citrate esters, which indicates the exceptional plasticization effects of

LAc and GAc compared to the widely used PLA plasticizers based on citrate esters such as TEC and ATBC. As can be seen in Table 4, the lowest T_g values are obtained with 20 wt.% LAc. These results are very interesting because they suggest a clear decreasing tendency of T_g, even though they are not reflected in increased elongation at break in plasticized formulations with 20 wt.% LAc or GAc. The T_g values obtained by REX with DCP are slightly higher than those obtained by conventional extrusion. This confirms the grafting of terpenoids onto the PLA backbone, which hinders chain motion and, subsequently, an increase in T_g. Similar behaviour can be observed for the cold crystallization temperature (T_{cc}). Both plasticizers provide increased chain mobility due to the internal lubricity effect; consequently, the cold crystallization is moved to lower temperatures. Neat PLA shows a cold crystallization peak temperature, T_{cc}, of 139.9 °C, and this is remarkably shifted down to values of 90 °C in formulations with 20 wt.% LAc and GAc. These results are in agreement with those reported by Chieng et al.

Fig. 3 Field-emission scanning electron microscopy (FESEM) images of the fractured samples from the tensile tests at 1000×. **a** PLA; **b** PLA-10LAc; **c** PLA-20LAc; **d** PLA-20LAc-DCP; **e** PLA-10GAc; **f** PLA-20GAc and **g** PLA-20GAc-DCP. Scale bar 10 μm
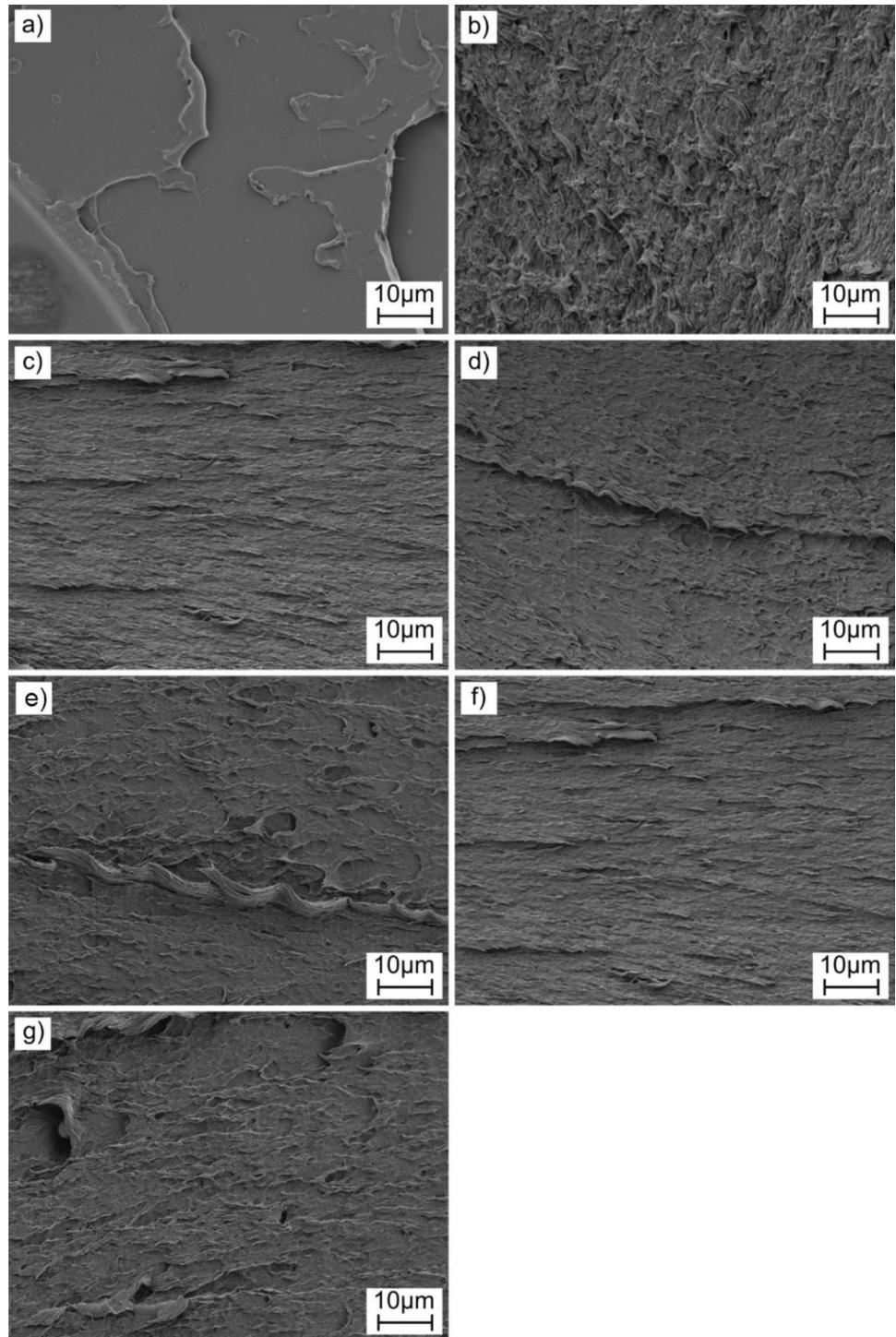
[52] in plasticized PLA formulations with 10 wt.% PEG with a decrease in T_{cc} by 50 °C regarding neat PLA. In this study, a remarkable decrease of almost 40 °C is obtained with 10 wt.% LAc. As mentioned above, the plasticizer enhances reduced interactions between polymer chains, thus leading to increase chain mobility. Accordingly, the cold crystallization peak temperature is moved to lower values. Moreover, as the chain mobility increases, the tendency of PLA polymeric chains are more readily to pack [43], and this is reflected by a noticeable increase in the cold crystallization enthalpy (ΔH_{cc}) that changes from 3.0 J/g for neat PLA up to values of 29.1 J/g for the PLA formulation containing 10 wt.% LAc. A similar increase in ΔH_{cc} has been reported by Xiao et al. [53], in plasticized PLA formulations with triphenyl
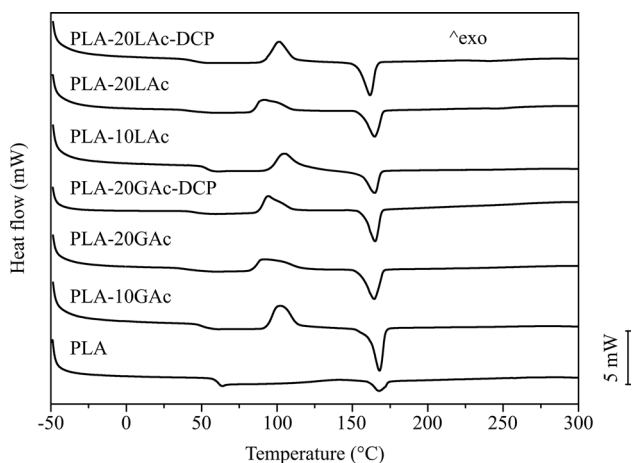
Fig. 4 Differential scanning calorimetry (DSC) thermograms of neat PLA and plasticized PLA formulations with terpenes by conventional and reactive extrusion, corresponding to the second heating cycle after removing thermal history

phosphate (TPP) as plasticizer. The degree of crystallinity (χ_{cmax}) was calculated by Eq. 7. This parameter is higher than PLA for all compositions. This is ascribed to improved segmental molecular mobility, as suggested by Clarkson et al. [48], in plasticized PLA formulations with PEG with the aid of nucleants derived from nanocelluloses. Another interesting finding is that much of this value corresponds to the cold crystallization process. Similar results have been reported by Xiao et al. [53] in plasticized PLA formulations with TPP plasticizer. The effect of the REX with DCP is also evident in T_{cc}. As expected, terpenoid grafting hinders chain mobility, and, subsequently, a noticeable increase in T_{cc} is also observed.

Additionally, the samples' thermal stability was measured by thermogravimetric analysis (TGA); the results are represented in Fig. 5 and Table 5. The thermal degradation of PLA occurred in a single step due to the chain scission with a maximum degradation rate temperature located at 373.8 °C [49]. The introduction of the plasticizer reduced the thermal stability of the plasticized PLA formulations due to the lower molecular weight of the terpenoid-based plasticizer.. The temperature at which a mass loss of 5 wt.%

Table 4 Summary of the DSC results for the PLA/terpene formulations

Code	T_g (ºC)	T_{cc} (ºC)	T_m (ºC)	ΔH_{cc} (J/g)	ΔH_m (J/g)	χ_c (%)
PLA	61.5 ± 0.5	139.9 ± 1.1	160.1 ± 1.2	3.0 ± 0.2	5.5 ± 0.3	2.7 ± 0.1
PLA-10LAc	50.4 ± 0.4	101.2 ± 1.3	161.0 ± 1.5	29.1 ± 0.8	34.3 ± 0.9	6.2 ± 0.2
PLA-20LAc	39.5 ± 0.3	90.4 ± 1.1	160.8 ± 1.4	27.7 ± 0.7	36.1 ± 0.8	11.3 ± 0.5
PLA-20LAc-DCP	45.3 ± 0.4	93.3 ± 1.0	163.1 ± 1.2	23.4 ± 0.7	29.7 ± 0.8	8.5 ± 0.1
PLA-10GAc	53.3 ± 0.3	103.6 ± 1.5	164.1 ± 1.0	15.2 ± 0.6	22.5 ± 0.7	8.7 ± 0.1
PLA-20GAc	42.2 ± 0.5	90.7 ± 1.4	163.5 ± 1.2	21.0 ± 0.5	28.5 ± 0.6	10.1 ± 0.1
PLA-20GAc-DCP	43.9 ± 0.5	101.1 ± 1.3	161.7 ± 0.8	27.1 ± 1.2	30.9 ± 0.9	5.1 ± 0.1

T_g glass transition temperature, T_{cc} cold crystallization temperature, T_m melting temperature, ΔH_{cc} cold crystallization enthalpy, ΔHm melting enthalpy, χ_c degree of crystallinity
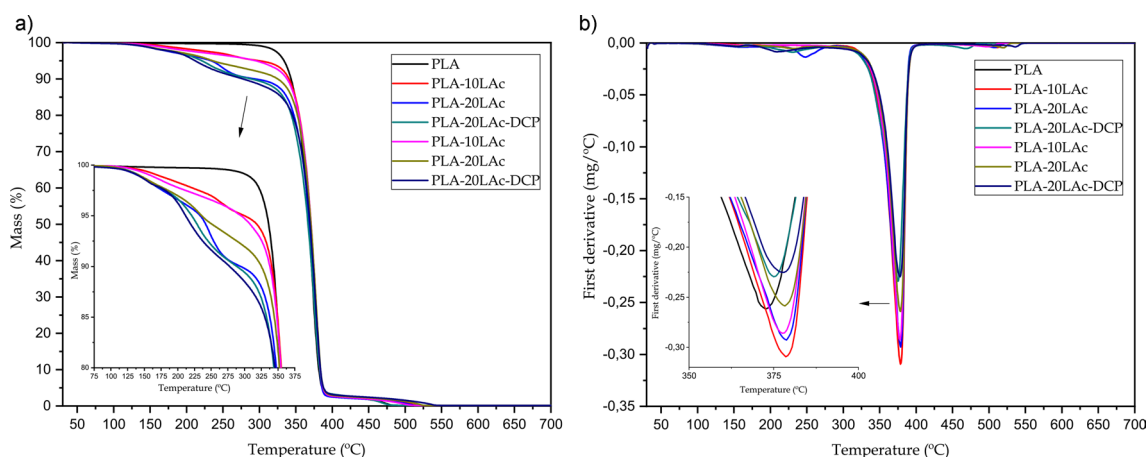

Fig. 5 Thermogravimetric (TGA) behaviour for the PLA/terpene formulations in terms of **a** mass loss and **b** first derivative of neat PLA and plasticized PLA formulations with terpenes by conventional and reactive extrusion

Table 5 Summary of the TGA results for the PLA/terpene formulations

Code	$T_{5\%}$ (ºC)	T_{deg} (ºC)
PLA	333.2 ± 1.2	373.8 ± 1.0
PLA-10LAc	292.2 ± 1.2	379.2 ± 1.2
PLA-20LAc	232.5 ± 1.1	378.7 ± 1.3
PLA-20LAc-DCP	218.1 ± 1.3	376.4 ± 1.1
PLA-10GAc	292.5 ± 1.0	378.3 ± 1.4
PLA-20GAc	232.4 ± 0.9	377.8 ± 1.2
PLA-20GAc-DCP	209.7 ± 0.8	377.2 ± 1.0

Initial temperature degradation at 5 wt.% loss ($T_{5\%}$), maximum rate degradation temperature (T_{deg}) and residual weight

occurs ($T_{5\%}$), changes from 333.2 °C to approximately 292 °C and 232 °C for the plasticized formulations with 10 wt.% and 20 wt.%, respectively of both LAc and GAc. Chieng et al. [52] observed a similar tendency in plasticized PLA formulations with low molecular weight PEG (200 g/mol). They reported a decrease in $T_{5\%}$ from 274.26 °C to 194.50 °C for a PEG-200 content of 10 wt.%. As the PEG-200 content increased, $T_{5\%}$ was proportionally reduced. In this study, LAc and GAc have the same molecular weight of 196.29 g/mol, and they provide an excellent plasticization effect on PLA, as demonstrated by tensile properties. Nevertheless, $T_{5\%}$ is reduced by 41 °C and 100 °C for LAc and GAc contents of 10 wt.% and 20 wt.%, respectively. From these results, the plasticized PLA formulations with 10 wt.% of either LAc or GAc seem to offer the best-balanced performance since the plasticization properties are exceptional and the degradation temperature is not remarkably reduced. This same behaviour has been reported by Maiza et al. [32] in plasticized PLA with TEC and ATBC, which are widely used as environmentally friendly plasticizers for PLA. For a 10 wt.% of TEC (Mw = 276.283 g/mol) and ATBC

(Mw = 402.484 g/mol), the $T_{5\%}$ was reduced from 348.94 °C (neat PLA) down to 303.54 °C and 313.63 °C, respectively. Therefore, the degradation temperatures obtained with LAc and GAc are comparable to those obtained with TEC and ATBC, thus suggesting similar performance. The maximum degradation rate of the formulations was similar to that of neat PLA. This was ascribed to independent degradation processes. Arrieta et al. [35] reported excellent plasticization properties in limonene-PLA films, but the onset degradation temperature (at a mass loss of 1%) was dramatically reduced from 322 °C to 109 °C for a plasticized formulation with 15 wt.% limonene, which is much volatile than the terpenoids used in this work due to its lower molecular weight.

Thermo-Mechanical Properties of Plasticized PLA Formulations with Terpenoids

The thermomechanical properties of the terpenoid-plasticized PLA formulations were measured through dynamic-mechanical thermal analysis (DMTA). In Fig. 6a, the storage modulus of the samples with increasing temperature is shown, while Fig. 6b gathers the evolution of the dynamic damping factor (tan δ) as a function of temperature of all developed formulations. The storage modulus, E', for neat PLA shows three different regions. Below 50 °C the storage modulus is almost constant. In the temperature range comprised between 55 and 75 °C, a dramatic decrease in E' (three-fold) occurs. This is associated with the glass transition region. After this, a plateau region with low E' values is observed and, finally, an increase in E' is observed in the temperature range of 80–90 °C, which is attributable to the cold crystallization process since this increase in crystallinity involves an increase in stiffness. As expected from DSC results, as the LAc and GAc content increases, the glass transition region and the cold crystallization process remarkably shift to lower temperatures due to increased segment chain
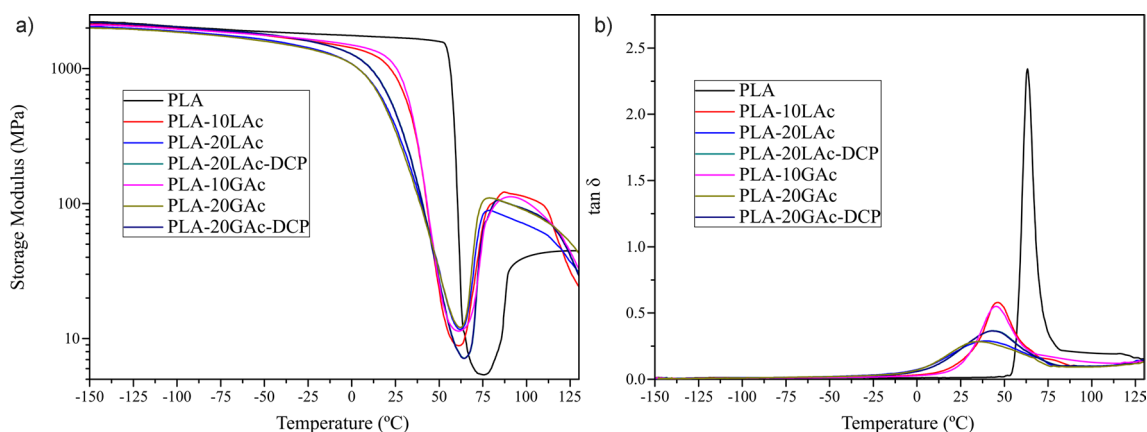

Fig. 6 Dynamic-mechanical thermal analysis (DMTA) behaviour of neat PLA and plasticized PLA formulations with terpenes by conventional and reactive extrusion. **a** storage modulus vs temperature and **b** dynamic damping factor (tan δ) vs temperature

motions. Another interesting finding is that the glass transition in neat PLA takes a very narrow temperature range, while this temperature range is broader for all plasticized formulations, as it can be seen in Fig. 6b. Table 6 summarizes some interesting parameters obtained by DMTA characterization. By taking the T_g as the peak temperature of the dynamic damping factor, a clear decreasing tendency is observed from 63 °C to 46.3 °C and 39.9 °C for the plasticized formulation with 10 wt.% and 20 wt.% LAc, respectively, thus corroborating the DSC results mentioned above. Similar T_g values are obtained for the plasticized system with GAc. As expected, REX with DCP provides a slight increase in T_g due to the grafting of terpenoids onto the PLA backbone, which restricts chain motion. Concerning the dynamic damping factor, the peak height is reduced, as observed in Fig. 6b. Moreover, it can also be observed that the tan δ peak is broader with increasing plasticizer content. This phenomenona was attributed to the fact that plasticized formulations have a wide range of relaxation times. Plasticizers have been reported to change the microheterogeneity of the plasticized PLA formulations with different compositions and interactions. In particular, hydrogen bonding and interactions with

oxygen atoms in plasticizer esters are responsible for this peak broadening. Shi et al. [50] also reported this peak broadening by adding different amounts of PEG into PLA formulations.

X-ray Diffraction Properties of Plasticized PLA Formulations with Terpenoids

The measured X-Ray diffraction pattern of the plasticized PLA formulations are presented in Fig. 7, and the main parameters obtained from XRD are gathered in Table 7. The main diffraction peak of the semicrystalline PLA is located at $2\theta = 16.35°$. This peak corresponds to diffraction planes (110)/(200) and α-type crystals [51, 52]. According to Bragg's equation, the distances between planes (d-spacing) were obtained. Very small changes in diffraction angles could be detectable, as seen in Table 7. The introduction of plasticizers, as mentioned above, enhanced the crystallization ability of PLA chains. As a result of the rearrangement of the polymer chains, the structure packs into a more compact structure that reduces de d-spacing between the crystalline planes [53]. Another phenomenon after plasticization with LAc and GAc is the increase of the d-spacing due to the

Table 6 Summary of the DMTA properties for the PLA/terpene formulations in terms of

Code	E' at − 20ºC (MPa)	E' at 25ºC (MPa)	T_g (ºC)
PLA	1814 ± 20	1698 ± 24	63.0 ± 0.5
PLA-10LAc	1605 ± 15	887 ± 10	46.3 ± 0.4
PLA-20LAc	1432 ± 11	376 ± 8	39.9 ± 0.4
PLA-20LAc-DCP	1605 ± 17	478 ± 6	43.5 ± 0.6
PLA-10GAc	1647 ± 18	1011 ± 17	45.8 ± 0.5
PLA-20GAc	1402 ± 25	345 ± 15	39.4 ± 0.5
PLA-20GAc-DCP	1610 ± 20	466 ± 9	43.1 ± 0.4

Storage modulus (E') and glass transition temperature (T_g)

Table 7 Summary of X-ray diffraction patterns (XRD) of neat PLA and plasticized PLA formulations with terpenes by conventional and reactive extrusion, in terms of the diffraction angle peak and d-spacing

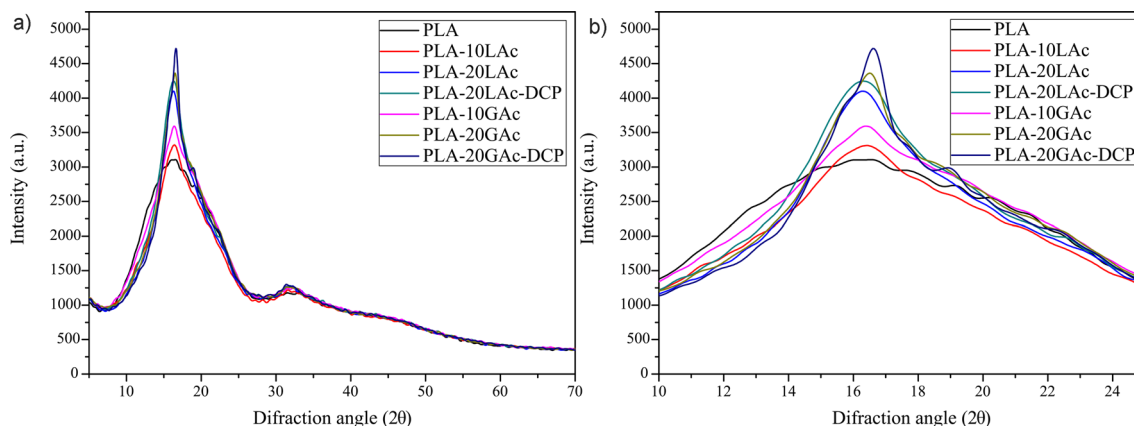| Code	2θ (°)	d-spacing (nm)
PLA	16.35	0.542
PLA-10LAc	16.40	0.540
PLA-20LAc	16.30	0.543
PLA-20LAc-DCP	16.35	0.542
PLA-10GAc	16.40	0.540
PLA-20GAc	16.50	0.537
PLA-20GAc-DCP	16.60	0.533

Fig. 7 X-ray patterns of neat PLA and plasticized PLA formulations with terpenes by conventional and reactive extrusion

placement of plasticizer molecules between the crystalline planes [54]. In this work, both phenomena occur, but they are overlapped, so the differences in the crystalline structure between neat PLA and the plasticized formulations with LAc and GAc are very small. The peak height is directly related to the degree of crystallinity. Therefore, as previously observed by DSC, neat PLA shows the lowest XRD peak height while this peak heigh is increased with increasing plasticizer content [55]. The introduction of terpenoid-based plasticizers resulted in an enhanced degree of crystallization.

Conclusions

Two terpenoids, namely linalyl acetate (LAc) and geranyl acetate (GAc), have proved to provide exceptional plasticization properties to poly(lactide) (PLA). In terms of mechanical properties, plasticized PLA formulations with 10 wt.% LAc offered the most remarkable improvement in elongation at break from 4.7% to 298.4%, which is 62.5 times much higher. The performance of these terpenoids is comparable, or even superior, to other conventional plasticizers for PLA, such as citrate esters, adipates and poly(ethylene glycol). These terpenoids have a solubility parameter close to that of PLA, which was reflected in low (< 1) relative energy dispersion (RED) values which suggested good miscibility. Thermal characterization by differential scanning calorimetry (DSC) revealed a remarkable decrease in the glass transition temperature from 61.5 °C to such low values of 39.5 °C for the plasticized formulation containing 10 wt.% LAc. Moreover, due to the particular structure of both terpenoids with several carbon–carbon double bonds, reactive extrusion (REX) with an organic peroxide, namely dicumyl peroxide (DCP), provides some grafting of the terpenoid molecules onto the PLA backbone. This phenomenon was confirmed by an increase in tensile strength (from values close to 14 MPa up to 16 MPa) and Young's modulus (from values around 200 MPa up to values near 400 MPa) and a slight increase in T_g compared to the respective formulation processed by conventional extrusion. Additionally, TGA results showed a clear decrease in $T_{5\%}$ for the plasticized samples, especially in the case with higher proportion of plasticizer (20 wt.%). This value decreased from a value of 300 °C for neat PLA down to approximately 210 °C for the plasticized samples. All in all, this research offers alternative plasticizers for environmentally friendly PLA formulations.

Declarations

Conflict of interest The authors declare no competing interests.

References

1. Jem KJ, Tan B (2020) The development and challenges of poly (lactic acid) and poly (glycolic acid). Adv Indus Eng Polym Res 3(2):60–70
2. Ramesh P, Vinodh S (2020) State of art review on Life Cycle Assessment of polymers. Int J Sustain Eng 13(6):411–422
3. Winnacker M, Rieger B (2016) Biobased polyamides: recent advances in basic and applied research. Macromol Rapid Commun 37(17):1391–1413
4. Zhang C, Madbouly SA, Kessler MR (2015) Biobased polyurethanes prepared from different vegetable oils. ACS Appl Mater Interfaces 7(2):1226–1233
5. Siracusa V, Blanco I (2020) Bio-polyethylene (Bio-PE), Bio-polypropylene (Bio-PP) and Bio-Poly(ethylene terephthalate) (Bio-PET): recent developments in bio-based polymers analogous to petroleum-derived ones for packaging and engineering applications. Polymers 12(8):1641
6. Yang Z et al (2020) Cost-effective synthesis of high molecular weight biobased polycarbonate via melt polymerization of isosorbide and dimethyl carbonate. Acs Sustain Chem Eng 8(27):9968–9979
7. Tsiropoulos I et al (2015) Life cycle impact assessment of bio-based plastics from sugarcane ethanol. J Clean Prod 90:114–127
8. Shen L, Patel MK (2008) Life cycle assessment of polysaccharide materials: a review. J Polym Environ 16(2):154–167
9. Valdes A et al (2015) Natural pectin polysaccharides as edible coatings. Coatings 5(4):865–886
10. Abedini F et al (2018) Overview on natural hydrophilic polysaccharide polymers in drug delivery. Polym Adv Technol 29(10):2564–2573

11. Song F et al (2011) Biodegradable soy protein isolate-based materials: a review. Biomacromol 12(10):3369–3380

12. Kowalczyk T et al (2014) Elastin-like polypeptides as a promising family of genetically-engineered protein based polymers. World J Microbiol Biotechnol 30(8):2141–2152

13. Rojas-Lema, S., et al., *"Faba bean protein films reinforced with cellulose nanocrystals as edible food packaging material".* Food Hydrocolloids, 2021. **121**, 107019

14. Montalvo-Paquini C et al (2018) Preparation and characterization of proteinaceous films from seven Mexican common beans (*Phaseolus vulgaris L.*). J Food Quality. https://doi.org/10.1155/2018/9782591

15. Pallos FM et al (2006) Thermoformed wheat gluten biopolymers. J Agric Food Chem 54(2):349–352

16. Mozejko-Ciesielska J, Kiewisz R (2016) Bacterial polyhydroxyalkanoates: Still fabulous? Microbiol Res 192:271–282

17. Rehm BHA (2010) Bacterial polymers: biosynthesis, modifications and applications. Nat Rev Microbiol 8(8):578–592

18. Seyednejad H et al (2011) Functional aliphatic polyesters for biomedical and pharmaceutical applications. J Control Release 152(1):168–176

19. Xu J, Guo B-H (2010) Poly(butylene succinate) and its copolymers: Research, development and industrialization. Biotechnol J 5(11):1149–1163

20. Woodruff MA, Hutmacher DW (2010) The return of a forgotten polymer-Polycaprolactone in the 21st century. Prog Polym Sci 35(10):1217–1256

21. Budak, K., O. Sogut, and U.A. Sezer, *A review on synthesis and biomedical applications of polyglycolic acid.* Journal of Polymer Research, 2020. **Doi:** https://doi.org/10.1007/s10965-020-02187-1

22. Robert JL, Aubrecht KB (2008) Ring-opening polymerization of lactide to form a biodegradable polymer. J Chem Educ 85(2):258–260

23. Razavi M, Wang S-Q (2019) Why is crystalline poly(lactic acid) brittle at room temperature? Macromolecules 52(14):5429–5441

24. Zhao X et al (2020) Super tough poly(lactic acid) blends: a comprehensive review. RSC Adv 10(22):13316–13368

25. Fortelny, I., et al., *Phase Structure, Compatibility, and Toughness of PLA/PCL Blends: A Review.* Frontiers in Materials, 2019. **6**.

26. Moradi, S. and J.K. Yeganeh, *Highly toughened poly(lactic acid) (PLA) prepared through melt blending with ethylene-co-vinyl acetate (EVA) copolymer and simultaneous addition of hydrophilic silica nanoparticles and block copolymer compatibilizer.* Polymer Testing, 2020. **91**: p. 106735

27. Quiles-Carrillo, L., et al., *Ductility and toughness improvement of injection-molded compostable pieces of polylactide by melt blending with poly(epsilon-caprolactone) and thermoplastic starch.* Materials, 2018. **11**(11).

28. Arrieta MP (2021) Influence of plasticizers on the compostability of polylactic acid. J Appl Res Technol Eng 2(1):1–9

29. Li D et al (2018) Preparation of plasticized poly (lactic acid) and its influence on the properties of composite materials. PLoS ONE. https://doi.org/10.1371/journal.pone.0193520

30. Athanasoulia I-G, Tarantili PA (2017) Preparation and characterization of polyethylene glycol/poly(L-lactic acid) blends. Pure Appl Chem 89(1):141–152

31. Maiza M, Benaniba MT, Massardier-Nageotte V (2016) Plasticizing effects of citrate esters on properties of poly(lactic acid). J Polym Eng 36(4):371–380

32. Tsou C-H et al (2018) Preparation and characterization of poly(lactic acid) with adipate ester added as a plasticizer. Polym Polym Compos 26(8–9):446–453

33. Guimaraes AC et al (2019) Antibacterial activity of terpenes and terpenoids present in essential oils. Molecules 24(13):2471

34. Barreto RSS et al (2014) A systematic review of the wound-healing effects of monoterpenes and iridoid derivatives. Molecules 19(1):846–862

35. Arrieta MP et al (2013) Characterization of PLA-limonene blends for food packaging applications. Polym Testing 32(4):760–768

36. Bruester B et al (2019) Plasticization of polylactide with myrcene and limonene as bio-based plasticizers: conventional vs reactive extrusion. Polymers 11(8):1363

37. Mangeon C et al (2018) Natural terpenes used as plasticizers for poly(3-hydroxybutyrate). Acs Sustai Chem Eng 6(12):16160–16168

38. Farah S, Anderson DG, Langer R (2016) Physical and mechanical properties of PLA, and their functions in widespread applications—A comprehensive review. Adv Drug Deliv Rev 107:367–392

39. Van Krevelen, D.W. and K. Te Nijenhuis, *Properties of polymers: their correlation with chemical structure; their numerical estimation and prediction from additive group contributions.* 2009: Elsevier.

40. Abbott, S., *Chemical compatibility of poly (lactic acid): A practical framework using Hansen solubility parameters.* Poly (Lactic Acid) Synthesis, Structures, Properties, Processing, and Applications, 2010: p. 83–95.

41. Gomez-Caturla, J., et al., *Improvement of Poly (lactide) Ductile Properties by Plasticization with Biobased Tartaric Acid Ester.* Macromolecular Materials and Engineering, 2023: p. 2200694.

42. Llanes, L.C., et al., *Mechanical and thermal properties of poly(lactic acid) plasticized with dibutyl maleate and fumarate isomers: Promising alternatives as biodegradable plasticizers.* European Polymer Journal, 2021. **142**.

43. Ge H et al (2013) Thermal, mechanical, and rheological properties of plasticized poly(L -lactic acid). J Appl Polym Sci 127(4):2832–2839

44. Liu H, Zhang J (2011) Research progress in toughening modification of poly(lactic acid). J Polym Sci, Part B: Polym Phys 49(15):1051–1083

45. Burgos N et al (2014) Synthesis and Characterization of Lactic Acid Oligomers: Evaluation of Performance as Poly(Lactic Acid) Plasticizers. J Polym Environ 22(2):227–235

46. Liao, J., et al., *Interfacial improvement of poly (lactic acid)/tannin acetate composites via radical initiated polymerization.* Industrial Crops and Products, 2021. **159**.

47. Rojas-Lema S et al (2021) Manufacturing and compatibilization of binary blends of polyethylene and poly (bulylene succinate) by injection molding. Journal of Applied Research in Technology & Engineering 2(2):71–81

48. Clarkson, C.M., et al., *Crystallization kinetics and morphology of small concentrations of cellulose nanofibrils (CNFs) and cellulose nanocrystals (CNCs) melt-compounded into poly(lactic acid) (PLA) with plasticizer.* Polymer, 2020. **187**.

49. Oliveira M et al (2016) The role of shear and stabilizer on PLA degradation. Polym Testing 51:109–116

50. Shi X et al (2015) Synergistic effects of nucleating agents and plasticizers on the crystallization behavior of poly (lactic acid). Molecules 20(1):1579–1593

51. Li F, Zhang C, Weng Y (2020) Improvement of the Gas Barrier Properties of PLA/OMMT Films by Regulating the Interlayer Spacing of OMMT and the Crystallinity of PLA. ACS Omega 5(30):18675–18684

52. Singh, S., M.L. Maspoch, and K. Oksman, *Crystallization of triethyl-citrate-plasticized poly(lactic acid) induced by chitin nanocrystals.* Journal of Applied Polymer Science, 2019. **136**(36).

53. Yu L et al (2008) Effect of annealing and orientation on microstructures and mechanical properties of polylactic acid. Polym Eng Sci 48(4):634–641

54. Meng Q, Heuzey MC, Carreau PJ (2014) Hierarchical structure and physicochemical properties of plasticized chitosan. Biomacromol 15(4):1216–1224

55. Ghasemlou M, Khodaiyan F, Oromiehie A (2011) Rheological and structural characterisation of film-forming solutions and biodegradable edible film made from kefiran as affected by various plasticizer types. Int J Biol Macromol 49(4):814–821